Fano resonance in electron transport through single dopant atoms

L. E. Calvet,[1,*] J. P. Snyder,[2] and W. Wernsdorfer[3]
[1]*Institut d'Electronique Fondamentale-CNRS UMR 8622, Université Paris-Sud, FR-91405 Orsay, France*
[2]*Volovox, LLC, Minnesota 55425, Minneapolis, USA*
[3]*Institut Néel, CNRS and Université J. Fourier, BP 166, FR-38042 Grenoble Cedex 9, France*
(Received 14 September 2010; revised manuscript received 28 January 2011; published 19 May 2011)

Antiresonances are observed in electron transport through a resonant dopant atom situated near a metal-semiconductor interface in a Schottky barrier metal-oxide-semiconductor field-effect transistor. The lineshapes do not significantly change in magnetic fields up to 5 T, but are modified by small dc bias voltages. We argue that these effects are the result of quantum interference between two tunneling paths and can be explained in the context of a Fano lineshape.

DOI: 10.1103/PhysRevB.83.205415 PACS number(s): 73.63.−b, 85.35.−p

Quantum interference has been a longstanding topic of research in mesoscopic physics because it probes the wave nature of electrons. While signatures of interference are observed in the magnetoresistance of confined nanostructures, giving rise to weak localization and universal conductance fluctuations,[1] even more intriguing are experiments in which interference can be directly measured. The most typical example is the Aharonov-Bohm ring, where electrons traversing two different paths interfere as a perpendicular magnetic field is varied.[2] In this paper, we show that a localized dopant in a semiconductor can act as an interferometer when two tunneling paths result in quantum interference, also known as the Fano effect.[3]

Unlike a discrete resonance in which the resulting characteristics exhibit Lorentzian peaks, the Fano effect results in a family of lineshapes depending on the phase difference between the two paths. They have been experimentally predicted and observed in a large variety of semiconductor heterostructures[4] and are of interest because the interference can provide valuable information about the coherence of the transport.[5,6] The Fano effect has been widely investigated in microfabricated quantum dots in which the design of the structure can serve as a playground for experimentalists. Researchers have investigated geometries in which the dot-lead coupling can be tuned,[7,8] in which an additional path has been included into the geometry[9] and embedded a quantum dot into an Aharonov-Bohm ring.[10]

Understanding the nature of quantum interference on the scale of a single nano-object, however, can be quite challenging. This topic is of great interest both theoretically[11] and experimentally[12–14] because observations can provide additional information about the measured object and serve as the basis of novel device concepts.[15,16] In this paper, we demonstrate quantum interference in the electrical transport through dopant atoms in silicon. There has been a definitive observation of Fano resonances between paths through two As atoms in a nanosized Si field-effect transistor (FinFET).[17] In the research considered here, we use micron size devices to demonstrate a quantum interference effect on a much smaller length scale, i.e., that approaching the Bohr radius of the atoms and thus similar to the length scale in single molecules.

I. EXPERIMENTAL DETAILS

We explore transport through dopant atoms located near the metallic contact in a *p*-type Schottky barrier metal-oxide-semiconductor field-effect transistor (SBMOSFET).[18] These devices have been widely researched in the past 15 years as an alternative to traditional MOSFETs for nanoscaled devices,[19] and a complementary metal-oxide-semiconductor (CMOS) technology has recently been demonstrated.[20] In the device, shown schematically in Fig. 1, metallic silicide source and drain electrodes are formed instead of the *p*-*n* junctions found in conventional MOSFETs. The variable temperature measurements indicate that, at low drain-source bias voltages V_{ds}, the transport is dominated by tunneling through the depletion region formed at the metal-semiconductor interface.[21] At low temperatures, resonant tunneling through individual atoms can be observed when the gate bias brings the energy level of an ionized dopant positioned close to the metal-semiconductor interface into resonance with the Fermi level.[18]

The SBMOSFETs used in this work consist of an *n*-type polysilicon gate, a *p*-doped substrate (5×10^{15} cm^{-3}), a 34-Å gate oxide, and 300-Å PtSi Schottky barriers.[22] In previous research, we explored the nature of transport through B and Pt dopants.[18,23,24] Measurements were performed using standard ac lock-in techniques in a dilution refrigerator with a base temperature of 50 mK. We apply magnetic fields up to 4.8 T in the plane parallel to the transport. We have observed antiresonances in five different devices, but, in this paper, we focus on one single device with dimensions of width and length = 3 and 0.5 μm, respectively, in which 10 resonant dips and 3 resonant peaks were observed.

II. RESULTS

Figure 2(a) shows differential conductance $\frac{\partial I_{ds}}{\partial V_{ds}}$ as a function of gate voltage $|V_g|$ at $V_{ds} = 0$ V and at an applied magnetic field $B = 2.7$ and 4.7 T. Two resonant peaks and 8 resonant dips, labeled consecutively a–h, are seen here. At larger magnetic fields, we observe that the peaks and dips are shifted either towards ($|V_g| > 0$) or away from ($|V_g| < 0$) the silicon valence band E_v, but that the lineshapes are not significantly altered. Figure 2(b) shows a three-dimensional plot of $\frac{\partial I_{ds}}{\partial V_{ds}}$ as a function of B. In order to emphasize the displacement of the lineshapes with magnetic field, we focus

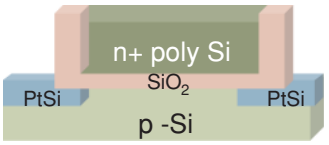

FIG. 1. (Color online) Schematic of the SBMOSFET (not drawn to scale). The source and drain tunneling contacts consist of the metal silicide PtSi. The gate is formed from a conventional metal-oxide-semiconductor (MOS) capacitor. The substrate is lightly doped (5×10^{15} cm^{-3}) with boron. The device operates in accumulation and transport is dominated by holes. The device dimensions used in this paper are width/length $= 3\ \mu$m$/0.5\ \mu$m.

on a smaller $|V_g|$ range that includes seven dips (dark lines) and one resonance (bright white line). Near $B = 0$ T, $\frac{\partial I_{ds}}{\partial V_{ds}}$ is strongly suppressed due to the superconducting gap formed when the PtSi electrodes become superconducting at temperatures below 1 K.[25] One observes only very small changes in the conductivity as the magnetic field is changed from 0.5 to 4.7 T. It is striking that both the dip and the peak positions exhibit either positive or negative monotonic displacements with magnetic field. To explore the nature of this magnetic field dependence, linear fits to the local maximum (peak) or minimum (dips) position as a function of magnetic field are plotted in dashed lines. The resultant slopes for each of the resonances and antiresonances are shown in Table I. In order to convert $|V_g|$ (V) into energy (eV), we use $\alpha = 0.155$ eV/V, as discussed in previous research.[24]

To understand the nature of the lineshapes, Fig. 3 plots the V_{ds} dependence of the peak (a) and a representative dip (c) at 4.7 T. We first note that the background conductance is suppressed at small V_{ds} due to the Altshuler-Aronov electron-electron correction of the tunneling density of states.[25] We observe, however, that at $V_{ds} = 0$ V, the resonant peak is suppressed to a greater extent than the background. To make this clearer, in Fig. 3(b), we scale several nonzero V_{ds} traces to the background conductance at $V_{ds} = 0$ V, $V_g = -1.951$ V. If the density of states correction simply increased the resonant tunneling proportional to the background, we expect that, for small V_{ds}, the resonant peaks would overlap. As $|V_{ds}|$ is increased, the resonance width should increase and the peak height should diminish due to standard Fermi level broadening. We do, indeed, observe that, at $V_{ds} > 0.2$ mV, the resonance is subject to the expected broadening; however, between 0 V to 0.2 mV, the peak height and width both increase.

Figure 3(c) explores the V_{ds} dependence of the antiresonances. While at $V_{ds} = 0$ V, the lineshape is mostly a dip below the background current, as V_{ds} is increased, the dip turns into an asymmetric lineshape containing both a resonant dip and peak. The most striking result is the reversal of the lineshape for negative and positive V_{ds}. To gain greater insight, in Fig. 3(d), we plot the evolution of dip c, scaled as in Fig. 3(b), by the background conductance at $V_{ds} = 0$ and $V_g = -1.913$ V. We observe that the lineshape changes from a sharp dip to an asymmetric lineshape with a dip and a peak, to finally something that is mostly a small resonant peak. We note that the other dips show similar behavior in that, as V_{ds} is increased, they transform into an asymmetric lineshape and then into either a very small resonant peak or disappear into the background current.

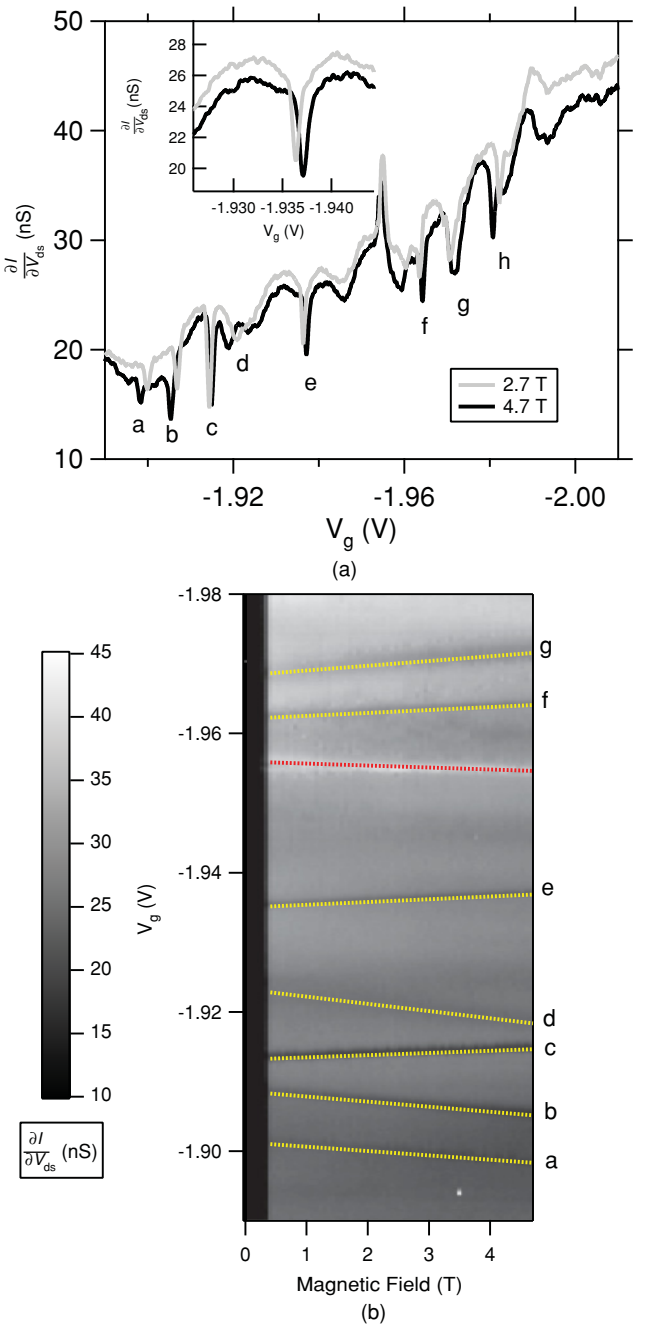

FIG. 2. (Color online) (a) Differential conductance $\frac{\partial I_{ds}}{\partial V_{ds}}$ vs gate voltage $|V_g|$ at $V_{sd} = 0$ V and magnetic fields $B = 2.7$ and 4.7 T at 50 mK. There are eight antiresonances, labeled a–h, and two resonant peaks. These lineshapes are shifted in energy (either to higher or lower $|V_g|$) with B, attributed mostly to the Zeeman effect. Although the magnitude of the differential conductance decreases slightly with field, there is not a substantial change in the lineshape. The inset shows a more detailed plot of dip e. (b) Three-dimensional plot of the $\frac{\partial I_{ds}}{\partial V_{ds}}$ showing the displacement of the lineshapes in (a) as a function of magnetic field. Here we use a small range of $|V_g|$ for clarity. The dotted lines are the linear fits obtained by extracting the local minimum (maximum) near the lineshape and the resultant slopes are reported in Table I.

TABLE I. Slopes of the magnetic field dependence of the peak or dip positions for the lineshapes observed in Fig. 2.

Lineshape	Slope (μeV/T)	Std. dev. (μeV/T)
a	−96.4	2.39
b	−111.8	1.49
c	48.8	1.44
d	−162.3	5.91
e	62.3	0.41
Peak 1	−44.33	0.98
f	64.5	0.74
g	106.8	4.84
h	−110.5	1.16
Peak 2	−55.5	0.98

III. DISCUSSION

We argue that the resonant dips are due to quantum interference. This is a very surprising result: we are able to probe coherent transport through a dopant atom in a device with relatively large dimensions (3 μm width by 0.5 μm length). Our attempts to explain this effect using other physical phenomena have proved untenable. For instance, the resonant dips can not be due to a thermoelectric effect because any such effects are not observable in an ac measurement in which the in-phase component with the same frequency as the excitation is measured.[26,27] These data can also not be explained by Pauli spin blockade in which two impurities coupled together[28,29] or a spin-polarized electrode[30,31] could result in significant current reduction. Such an effect would result in rectifying behavior as a function of bias voltage direction. While we do observe changes in the lineshape with bias direction, we do not report a greater suppression of the resonance for one particular polarity. To fully appreciate the experimental data in the previous section, it is first necessary to understand the nature of the resonant states and the shift in energy of the lineshapes with magnetic field.

A. Origin of the resonances and antiresonances and magnetic field dependence

In previous research, we have explored resonant peaks due to Pt (Ref. 24) and/or B atoms[18,23] that are present in the device. We investigated the Zeeman effect as a function of magnetic field and excited state spectroscopy with V_{ds}. In Table I, we recognize many of the slopes from this previous research. Antiresonance *d,* for instance, shows a slope indicative of a $m_j = 3/2$ and $g = 1.86 \pm 0.07$, consistent with boron atoms.[18,23] For the impurity shown in the inset of Figs. 3(c) and 3(d) (dip c), the magnetic field dependence [Fig. 2(b)] is -48.825 ± 1.44 μeV/T. Assuming a 1/2 spin, this results in a g factor of 1.68 ± 0.05, which is within the experimental accuracy of the 1.38 ± 0.43 g factor from previous research,[24] and thus this dopant is likely to be a double donor of Pt. We note that the slopes of dips a, b, g, and h and the two peaks have previously been reported as related to Pt atoms.[24] The remaining dips (e and f) are likely due to boron atoms.

Compared with spectroscopy of small microfabricated quantum dots,[32,33] the charging energies of typical dopants in silicon are large. Pt is known to have three charged states located at approximately E_c −0.243 eV (single acceptor), $E_v + 0.330$ eV (single donor), and $E_v + 0.1$ eV (double donor), where $E_{x=c,v}$ is, respectively, the conduction or valence band.[34] Defects of Pt involving other atoms such as H and O have similarly large charging energies between different states.[34] Researchers have investigated B in bulk samples using piezo,[35] electron paramagnetic resonance,[36] and infrared[37] spectroscopies to investigate the energy spectrum of the A^0 (located 0.045 eV above E_v) and excited states (located between 12–2 meV above E_v). To access the second bound hole state A^+, phonon spectroscopy has been used.[38] This state is very close to the valence band edge (2 meV) and thus investigations are quite limited. Recent research has explored the A^+ state using transport spectroscopy of a δ-doped silicon layer.[39] We have previously investigated the ground state of B dopants,[18,23] but are not able to determine the ionization energy using our experimental method. Another group has

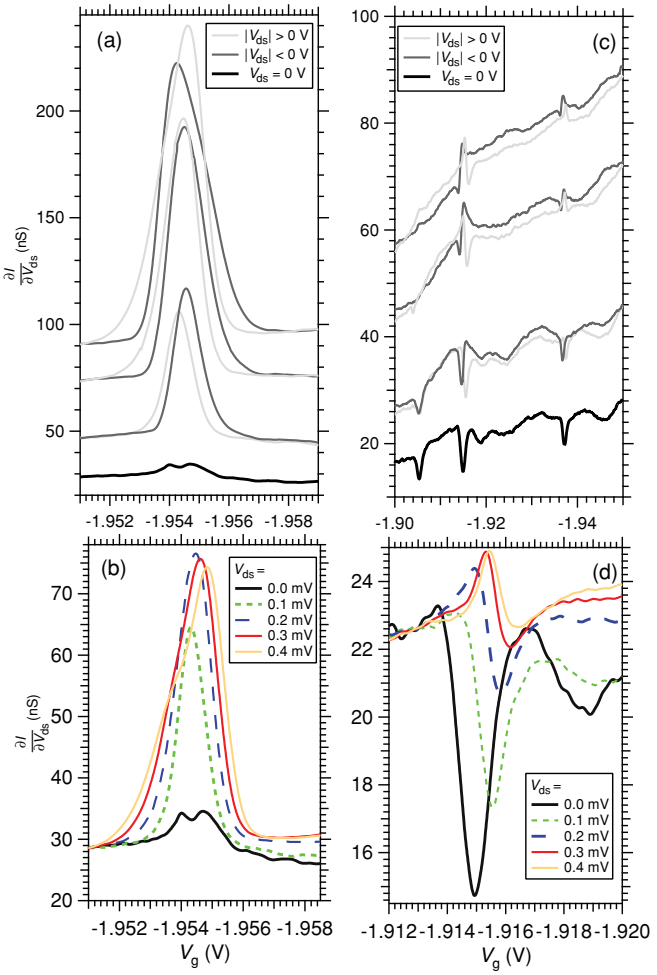

FIG. 3. (Color online) Changes in the lineshape at different V_{sd} of a resonant peak (a) and (c) and dip c (b) and (d). In both (a) and (c), the $\frac{\partial I_{ds}}{\partial V_{ds}}$ of the $V_{ds} = 0$ V curve is significantly suppressed compared to higher bias. This suppression of the background current is due to electron-electron interactions. In (b) and (d), the lineshapes are scaled, respectively, by the $\frac{\partial I_{ds}}{\partial V_{ds}}$ at $V_{ds} = 0$ V, $V_g = -1.951$ V, and $V_{ds} = 0\,V$, $V_g = -1.913$ V. However, as shown in (b) and (d), the lineshapes do not scale in the same way as the background. All curves are shown at 50 mK and at 4.7 T.

investigated single[40,41] and coupled acceptors[42] in nanoscale silicon-on-insulator (SOI) FET devices and found a much smaller ionization energy (10 meV) than the bulk value. This is likely due to the position of the dopant close to the SOI interface.[43] Other researchers who have investigated single donors of small silicon SOI MOSFETs have found values similar to the bulk,[44] exceeding the bulk up to 2× (Ref. 43) or less than the bulk down to 0.5×.[45] We estimate that the charging energy of individual dopants in silicon should be $\geqslant$ 20 meV, which is at least an order of magnitude larger than the charging energy of small microfabricated quantum dots.[32,33] We thus see that the energy scale represented in Fig. 2, which is ∼14 meV, is small on the energy scale of the charging energies of typical dopants in silicon. If the individual resonances and antiresonances reported here are related to single atoms or a single atom coupled to H or O, the different levels should, therefore, not correspond to levels of the same dopant. There are two other possibilities that we briefly consider: coupled atoms and the creation of a small quantum dot based on a cluster of dopants.

We can compute an average number of B atoms near the metal-semiconductor interface (about 1.5 dopants for every 1 μm of device width) based on the device dimensions and background doping. Such dopants are spread out randomly over the entire micron size device width, and it can be expected that most resonant boron atoms are uncoupled with each other. However, Pt atoms present another problem because the number of atoms that have diffused from the metal-semiconductor interface can vary widely[46] and TEM observations show the occasional formation of Pt clusters.[47] We thus consider the possibility that many Pt atoms could form a multiatom cluster or a few-atom coupled state.

Forming a quantum dot from a cluster of dopants was recently considered both experimentally and theoretically by the Nottingham group.[48,49] This research showed that the deepest quantum well was created by about 10 randomly placed Mn atoms in GaAs quantum wells confined in about ∼10 nm. Generation of quantum dot formed from a cluster of atoms resulted in a very distinguishable Fock-Darwin-type energy spectrum in magnetic field due to orbital effects of filling additional electrons. This spectrum is taken by assuming a circular confining potential and solving the Schrodinger equation. The eigenenergies are given by

$$E_{n,l} = \left[(2n + |l| + 1)\hbar \left(\omega_0^2 + \frac{\omega_c^2}{4} \right)^{\frac{1}{2}} - \frac{1}{2}\hbar l \omega_c \right], \quad (1)$$

where n and l are the radial and angular momentum quantum numbers, ω_0 is the oscillator frequency, and $\omega_c = eB/m^*$ is the cyclotron frequency. This spectrum has some very well-defined magnetic features; however, depending on the confinement of the dot, they can be spread out, and depending on the charging energy, they may become truly evident only at high magnetic fields. We now consider the relevant energy scales in our system.

For our system, the ionization energies of the relevant single atoms are between 50–100 meV below E_v, which would result in quantum dot clusters with the smallest addition energies ∼4–20 meV and, thus, a Fock-Darwin spectra observable within the 5-T magnetic field dependence of the experiment. In the silicon valence band, the energy scales of the Fock-Darwin spectra are considerably different from GaAs. First, the contribution of the cyclotron energy $\hbar\omega_c/2B \approx 115$ μeV/T (assuming an effective mass $m^* = 0.5m_e$) is much smaller than the expected confinement energy $\hbar\omega_0 \geqslant 4$ meV, so that Eq. (1) can be approximated as $E_{n,l} \approx [(2n + |l| + 1)\hbar\omega_0 - \frac{1}{2}\hbar l\omega_c]$. For small values of l, the magnetic field dependence is the same order as the Zeeman energy $\Delta E_z/B = g m_j \mu_B \approx 58\mu$eV/T for $g = 2$ and $m_j = 1/2$. We must therefore include ΔE_z when considering such orbital effects.

The $|V_g|$ range in Fig. 2(b) corresponds to 14 meV. We can not exclude orbital effects and the presence of clusters from these data, however, we can not account for all of the resonance and antiresonances by one cluster of defects forming a quantum dot. Specifically, the peak position versus magnetic field slopes should be larger with increasing filling, but, in Table I, the slopes cluster around ±100 and ±50 μeV/T. We note that dips c and d might be attributed to the $l = \pm 1$ states of a cluster, but in this energy window, we could not attribute any of the other structures to either the $l = 0$ or ± 2 states. Precise assignment here is further complicated because the slope of dip d could also be attributed to the ground state of a boron acceptor impurity.[18,23]

An additional possibility is that the magnetic field orientation is not suitable for observing orbital effects and that some of the slopes in Table I are due to successive spin filling of a small impurity quantum dot.[32,50] Unlike microfabricated quantum dots in GaAs, quantum dots in silicon are much less prone to the overall diamagnetic shift observed on the different addition energies. This shift becomes important when the charging energy is comparable to the diamagnetic energy

$$\frac{e^2 B^2 r^2}{8m^*} \approx \frac{e^2}{4\pi\varepsilon_s r},$$

where r is the overlap of the wave function and the electrode. The ∼10× larger effective mass in silicon renders this effect negligible in our system. We thus can compare the shifts of each of the energies directly without having to compare peak spacings. While one expects the typical Pauli filling, the research in microfabricated quantum dots has shown that deviations are possible, providing evidence for higher spin states. Successive spin filling should follow $\pm g\mu_B$ and, therefore, we only consider slopes in Table I in which the absolute values are approximately equal. If we interpret dips a, b, g, and h in this context, we would have successive spin filling of (↓, ↓, ↑, ↓).

Next, we consider the possibility of Pt atoms forming clusters of a few atoms so that a single defect can result in several levels. Such clusters were recently considered in an extension of scanning charge accumulation imaging.[51] In transport, other researchers have discussed the characteristics of donor molecules[52] and explored the effect of interacting impurities.[53–55] All of these investigations demonstrate that a coupled impurity state (containing the same species of impurity) in which two atoms are close together results in a large additional charging energy associated with the second state. This second state is situated at much higher energy, ranging from 1 to 4× the binding energy depending on the distance between the two impurities. In order to observe the effects of interacting impurity on a resonant level, it is

necessary to consider the V_{ds} dependence and investigate the nature of excited states. Alternatively, by modifying a perpendicular magnetic field, the overlap between the impurities can be modified. The previous research that explored interacting impurities in electron transport[53–55] focused on the case where the impurities were separated by large distances. Essentially, if the impurities are close enough together, they are difficult to distinguish from the single impurity case, especially at $V_{ds} = 0$ V and in parallel magnetic fields. In the next section, we discuss how the fact that the quantum interference does not change in magnetic fields up to 5 T implies that the path length is quite small ($\ll$32 nm). If the interference originates from two paths through two different impurities, these impurities are necessarily situated very close together. We can not distinguish if a given resonance or antiresonance in Fig. 2(b) is due to a coupled or a single impurity given the data reported here. However, if there are coupled impurities, not all the resonances in Fig. 2 can originate from one coupled system because the transport window is too small.

Our system is unique compared to previous investigations in that the device contains two known species of dopants: single B acceptors and double Pt donors. Transport is close to the valence band and both atoms can be viewed as binding holes. However, the acceptor site is initially charged negatively and becomes neutral and the Pt site is initially charged positively and an additional positive charge is added. If these two species are close enough to be coupled, then the occupation of one level will result in the other level moving away from the valence band (to lower energy). Coupling between two states of an acceptor (double donor) would thus result in a *decrease* of the ionization of one of the states when the other level becomes occupied. In this context, two of the levels in Fig. 2 could be related to such coupled atoms.

In summary, we have seen in this section that the levels in Fig. 2 have several possible origins. They can originate from Pt or *B* atoms that are isolated or coupled either with each other or with an atom of the same species or with O or H. It is possible that two or three of the levels in Fig. 2 belong to the same coupled atoms. Another possibility is that a small cluster containing a few impurities forms a very small quantum dot and several of the levels belong to the same cluster.

Without additional spectroscopy experiments, one can not precisely classify the origin of each resonance in Fig. 2. As we have shown by comparing the values in Table I with our earlier work,[18,23,24] the identity of a given state, as determined by the change of its peak position at $V_{ds} = 0$ V as a function of magnetic field, does not determine whether it will be observed as a resonant dip or a resonant peak. What is clear from this analysis is thus that the presence of antiresonances due to single atoms, coupled atoms, or a small quantum dot based on a few dopants is a robust effect in these devices.

B. Interpretation of the antiresonances as quantum interference

We now consider how an antiresonance might occur. To simplify the exposition, we assume for the moment that the resonant path is due to a single atom, although, from our discussion above, this may not be true. What is surprising is that the dip goes *below* the apparent background current. One naively expects that the background tunneling current in the device is due to transport along the entire width. Thus, if there is a destructive interference through a resonant level, it could not go below this incoherent background current. However, at low temperatures in a relatively small Schottky barrier like the one we have here, the depletion region is nonuniform. Near a dopant level, direct tunneling is significantly enhanced because the barrier height and width are modified by the electrostatic potential of the charge. As a result, the width of the Schottky barrier is broken up into regions of high conduction, near a resonant atom, and regions of low conduction, where there are no dopant levels. In order to observe interference effects, when the equilibrium Fermi level is near resonance with an atomic level, the dominant transport mechanism must be coherent. When there is destructive interference, the path through the atom is blocked and the current can be significantly decreased because one of the few paths through the entire barrier width has been blocked off.

Evidence for this effect can be found by looking at the amount by which the antiresonances dip below the background as a function of $|V_g|$. When transport through a quantum dot is strictly determined by the Fano resonance, e.g., there are no other transport paths, the distance from the bottom of the dip to zero can be indicative of the coherence of the transport.[5] Here the dip can only go so low until the conductance from other paths through the barrier becomes important. However, as $|V_g|$ is increased, we expect that direct tunneling through the entire barrier width will increase and, correspondingly, the difference between regions of high conductance and low conductance will decrease. Thus, the general trend of how much the dips go below the background should be inversely proportional to $|V_g|$. Figure 4 shows the percent change of the total current for each of the antiresonances. Indeed, the general trend is that the number and strength of the antiresonances decreases as $|V_g|$ is increased.

Assuming that electron-electron interactions can be neglected,[56] coherent transport through the impurity can be described by the Landauer-Buttiker formalism[1] in which a

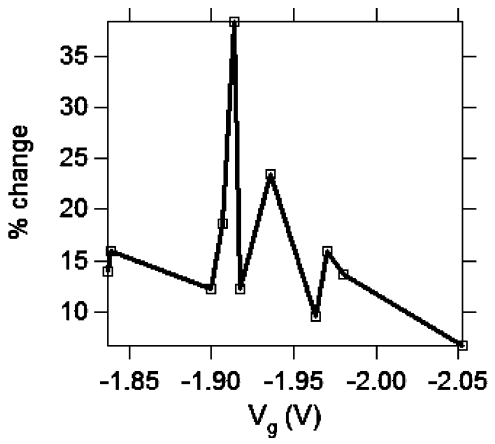

FIG. 4. For each of the antiresonances in Fig. 2(a) at 4.7 T, we calculate the percentage the differential conductance dips below the accompanying shoulder. The frequency and percent change of the differential conductance decreases as $|V_g|$ increases. This provides evidence that the background current in the channel is increasingly dominated by incoherent direct tunneling through the barrier rather than "hot spots" resulting from resonant levels.

scattering transmission coefficient is used to describe the current. When quantum interference comes into play, the typically Lorentzian transmission coefficient can be replaced with the Fano transmission amplitude describing interference between two paths:[7]

$$T(E, V_{ds}) = t_{nr} \frac{|2\varepsilon + q|^2}{4\varepsilon^2 + 1}, \quad (2)$$

where t_{nr} is the transmission probability of the nonresonant path (likely to be direct tunneling), $\varepsilon = E - E_{\text{res}}/\Gamma$ is the change in energy near the resonance, and q is the asymmetry factor related to the cotangent of the phase difference δ between the two paths and proportional to the transmission probability of resonant tunneling t_{rt} over that for nonresonant tunneling:

$$q = \cot\delta \propto \frac{t_{rt}}{t_{nr}\Gamma}.$$

For $q = 0$, the lineshape exhibits a resonant dip, for large q the Lorentzian is recovered, and, at intermediate values, asymmetric lineshapes are observed.

The data in Fig. 3 have a relatively simple interpretation in this context. For the resonant tunneling peak in Figs. 3(a) and 3(b), we observe that the resonance is initially enhanced as $|V_{ds}|$ is increased. This is unusual because typically increasing $|V_{ds}|$ introduces thermal energy that will broaden the resonance and not result in a more pronounced resonant tunneling. Here, however, tunneling into the semiconductor channel is strongly suppressed at zero bias;[25] thus, introducing a small bias voltage effectively enhances all transport into the semiconductor channel. We note that a similar suppression near $|V_{ds}| = 0$ V has been described theoretically.[57] Pure resonant tunneling can be described by a Breit-Wigner lineshape $T = \Gamma_{MD}\Gamma_{DS}/[(E - E_{\text{res}})^2 + (\Gamma_{MD}/2 + \Gamma_{DS}/2)^2]$, where $\Gamma_{x=MD,DS}$ are, respectively, the leak rates from the metal to the dopant and the dopant to the semiconductor. In an SBMOSFET, the leak rates are determined by the depletion potential resulting from the metal-semiconductor interface and are thus highly asymmetric. As a result, removing the zero bias current suppression unequally changes these two parameters. The leak rate closest to the semiconductor will experience the largest change. If the dopant is thus very close to the metal, then there will be an enhancement in the total resonant tunneling component. If the total transmission coefficient, which includes the probability for nonresonant and resonant tunneling through the atom, is such that resonant tunneling is much larger than the nonresonant component, increasing the bias voltage will result in a stronger Lorentzian peak.

If, however, the transmission coefficient for resonant tunneling is smaller or comparable to that of the nonresonant component, then the resonance exhibits a Fano lineshape and the bias voltage modifies its parameters, as in the data in Fig. 3(d). Effectively, by changing the bias voltage, one is tuning one of the leak rates of the resonant tunneling component, increasing its importance relative to the nonresonant component. Figure 5(a) shows the fits to the Fano expression for the resonance in Fig. 3(d). Figure 5(b) plots the fitted expression for the asymmetry parameter q as a function of bias voltage. Most interestingly, the lineshape goes from having almost complete destructive interference ($q = 0$) to constructive interference ($q = \pm 1$). Because the leak rates are modified by the bias voltage and not more directly by adjusting a tunnel barrier,[7,8] an additional effect related to the *direction* of $|V_{ds}|$ is observed. In Fig. 5(b), the sign of q reverses from positive to negative with bias voltage direction. The explanation for this is that the asymmetry parameter q is a measure of the phase difference between the direct and resonant tunneling paths. Thus, applying a bias voltage in the positive or negative direction is equivalent to shifting the phase by 180°.

One surprising feature of these data is that the lineshape changes form with bias voltage but not with magnetic field. One possibility is that the path length of the interference is smaller than the corresponding magnetic field length we have accessed. In order to change the interference by one complete cycle, the magnetic field flux $\Phi = BS$, where S is the surface area of the path, must be of order $\frac{h}{e}$. At 5 T, this implies a maximum surface area of 8.27×10^{-16} m^2 or, assuming a circular path, a diameter of order 32 nm. The fact that we see no significant change implies that the interference path is likely to be much smaller than this. This diameter is still much larger than the typical ~2-nm Bohr radius for a shallow dopant level near the valence band.[58]

Finally, we consider briefly the origin of the nonresonant path. There are several possibilities including (1) tunneling through a nearby dopant(s), (2) direct tunneling due to the proximity of the atom to the metallic electrode, (3) enhanced direct tunneling through surface states present at the metal-

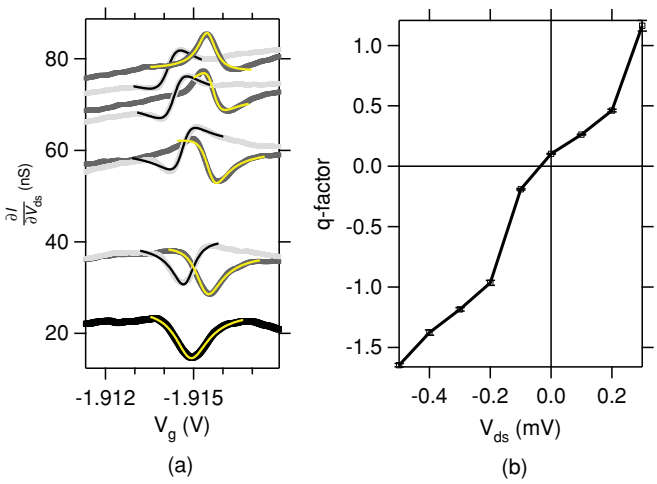

FIG. 5. (Color online) (a) We fit the Fano lineshape [Eq. (2)] to dip c in Fig. 3 at 4.7 T and 50 mK. The value of the V_{ds} from bottom to top is 0, ±0.1, ±0.2, ±0.3, and ±0.4 mV. Note that the curves are NOT offset. The $V_{ds} = 0$ V curve is plotted in black with the fit indicated in gray, the positive V_{ds} curves are plotted dark gray with fits in light gray and the negative V_{ds} curves are plotted in light gray with fits in dark gray. (b) Plot of the asymmetry factor q as a function of bias voltage V_{ds}. At $V_{ds} = 0$ V, we observe an antiresonance, corresponding to an asymmetry parameter q close to 0, and indicative of destructive interference. For $V_{ds} > 0$ V, we find positive q values and, for $V_{ds} < 0$ V, negative q values, as might be expected if the interference is changed by a 180° phase shift. As $|V_{ds}|$ is increased, the resonant tunneling component becomes more important and the interference becomes increasingly constructive, indicated by $q = 1$. Note that the standard deviation of the q-parameter fit is indicated by error bars, which demonstrate the robustness of the changes with $|V_{ds}|$.

semiconductor surface, and (4) an additional current path within the atom due to the resulting physical structure within the silicon lattice. The very fact that we observe resonances with different magnetic field dependences may indicate that the dopants do not all exhibit quantum interference of exactly the same origin and we, therefore, can not exclude any of these options without further experimental investigations. We mention that, in the first case, the second atom must be in very close proximity because of the very small path length implied by the magnetic field dependence. Two possible ways to address this issue are to explore the temperature dependence of the interference[8] or how the quantum interference of dopant levels with different magnetic field dependences changes as the superconductivity in the PtSi contacts is suppressed.[59]

IV. SUMMARY

We have explored antiresonances in the transport through dopant atoms located near the metal in a Schottky barrier MOSFET. We find that the lineshapes can be explained in terms of quantum interference via a Fano lineshape. We observed significant changes in the lineshapes with applied bias voltage that are due to changes in the resonant tunneling component of the interference. Finally, because the lineshapes exhibit very little change in magnetic fields up to 5 T, we argue that the quantum interference path must be very small. The data show that this system is capable of demonstrating interference on a very small length scale and thus provide a novel test bed for exploring coherence with a small number of atoms.

ACKNOWLEDGMENTS

The idea of observing Fano resonances in Schottky barrier MOSFETS originates from research at Yale University with M. Reed and R. Wheeler. L.E.C. thanks M. Jang, K. Kang, E. Hoffman, and H. Linke for invaluable discussions.

*laurie.calvet@u-psud.fr

[1] S. Datta, *Electronic Transport in Mesoscopic Systems* (Cambridge University, Cambridge, UK, 1995), Chap. 5.
[2] S. Washburn and R.A. Webb, Adv. Phys. **35**, 375 (1986).
[3] U. Fano, Phys. Rev. **124**, 1866 (1961).
[4] A. E. Miroshnichenko, S. Flach, and Y. S. Kivshar, Rev. Mod. Phys. **82**, 2257 (2010).
[5] A. A. Clerk, X. Waintal, and P. W. Brouwer, Phys. Rev. Lett. **86**, 4636 (2001).
[6] J. U. Nockel and A. D. Stone, Phys. Rev. B **50**, 17415 (1994).
[7] J. Göres, D. Goldhaber-Gordon, S. Heemeyer, M.A. Kastner, H. Shtrikman, D. Mahalu, and U. Meirav, Phys. Rev. B **62**, 2188 (2000).
[8] I.G. Zacharia, D. Goldhaber-Gordon, G. Granger, M.A. Kastner, Y. B. Khavin, H. Shtrikman, D. Mahalu, and U. Meirav, Phys. Rev. B **64**, 155311 (2001).
[9] A. C. Johnson, C. M. Marcus, M. P. Hanson, and A. C. Gossard, Phys. Rev. Lett. **93**, 106803 (2004).
[10] K. Kobayashi, H. Aikawa, S. Katsumoto, and Y. Iye, Phys. Rev. Lett. **88**, 256806 (2002); Phys. Rev. B **68**, 235304 (2003).
[11] See, for instance, T. Hansen, G. C. Solomon, D. Q. Andrews, and M. A. Ratner, J. Chem. Phys. **131**, 194704 (2009); D. Darau, G. Begemann, A. Donarini, and M. Grifoni, Phys. Rev. B **79**, 235404 (2009), and references therein.
[12] C. Patoux, C. Coudret, J. P. Launay, C. Joachim, and A. Gourdon, Inorg. Chem. (Washington, DC) **36**, 5037 (1997).
[13] M. Arndt, O. Nairz, J. Vos-Andreae, C. Keller, G. van der Zouw, and A. Zeilinger, Nature (London) **401**, 680 (1999).
[14] M. Mayor, H. Weber, J. Reichert, M. Elbing, C. von Hänisch, D. Beckmann, and M. Fischer, Angew. Chem., Int. Ed. **42**, 5834 (2003).
[15] D. M. Cardamone, C. A. Stafford, and S. Mazumdar, Nano Lett. **6**, 2422 (2006).
[16] D. Darau, G. Begemann, A. Donarini, and M. Grifoni, Phys. Rev. B **79**, 235404 (2009).
[17] J. Verduijn, G. C. Tettamanzi, G. P. Lansbergen, N. Collaert, S. Biesemans, and S. Rogge, Appl. Phys. Lett. **96**, 072110 (2010).
[18] L. E. Calvet, R. G. Wheeler, and M. A. Reed, Phys. Rev. Lett. **98**, 096805 (2007).
[19] J. M. Larson and J. P. Snyder, IEEE Trans. Electron. Devices **53**, 1048 (2006).
[20] M. Jang, Y. Kim, M. Jeon, C. Choi, I. Baek, S. Lee, and B. Park, IEEE Trans. Electron. Devices **53**, 1821 (2006).
[21] L.E. Calvet, R.G. Wheeler, and M.A. Reed, Appl. Phys. Lett. **80**, 1761 (2002).
[22] C. Wang, J. P. Snyder, and J. R. Tucker, Appl. Phys. Lett. **74**, 1174 (1999).
[23] L.E. Calvet, R.G. Wheeler, and M.A. Reed, Phys. Rev. B **76**, 035319 (2007).
[24] L. E. Calvet, J. P. Snyder, and W. Wernsdorfer, Phys. Rev. B **78**, 195309 (2008).
[25] L. E. Calvet, J. P. Snyder, and W. Wernsdorfer, Phys. Rev. B **78**, 193309 (2008).
[26] L.W. Molenkamp, H. van Houten, C.W.J. Beenakker, R. Eppenga, and C.T. Foxon, Phys. Rev. Lett. **65**, 1052 (1990); H. van Houten, L. W. Molenkamp, C. W. J. Beenakker, and C. T. Foxon, Semicond. Sci. Technol. **7**, B215 (1992).
[27] G. Granger, J. P. Eisenstein, and J. L. Reno, Phys. Rev. Lett. **102**, 086803 (2009).
[28] K. Ono, D. G. Austing, Y. Tokura, and S. Tarucha, Science **297**, 1313 (2002).
[29] A. C. Johnson, J. R. Petta, C. M. Marcus, M. P. Hanson, and A. C. Gossard, Phys. Rev. B **72**, 165308 (2005).
[30] P. Hawrylak, C. Gould, A. Sachrajda, Y. Feng, and Z. Wasilewski, Phys. Rev. B **59**, 2801 (1999).
[31] D. Kupidura, M. C. Rogge, M. Reinwald, W. Wegscheider, and R. J. Haug, Phys. Rev. Lett. **96**, 046802 (2006).
[32] D. S. Duncan, D. Goldhaber-Gordon, R. M. Westervelt, K. D. Maranowski, and A. C. Gossard, Appl. Phys. Lett. **77**, 2183 (2000).
[33] L.P. Kouwenhoven, D.G. Austing, and S. Tarucha, Rep. Prog. Phys. **64**, 701 (2001).
[34] See, for instance, Chapter 9 in A. Resende, Ph.D. thesis, University of Exeter, 1999, and references therein.
[35] H. R. Chandrasekhar, P. Fisher, A. K. Ramdas, and S. Rodriguez, Phys. Rev. B **8**, 3836 (1973).

[36]G. Feher, J. C. Hensel, and E. A. Gere, Phys. Rev. Lett. **5**, 309 (1960).
[37]D. Karaiskaj, T. A. Meyer, M. L. W. Thewalt, and M. Cardona, Phys. Rev. B **68**, 121201(R) (2003).
[38]W. Burger and K. Lassmann, Phys. Rev. Lett. **53**, 2035 (1984).
[39]J. Caro, I.D. Vink, G.D.J. Smit, S. Rogge, T.M. Klapwijk, R. Loo, and M. Caymax, Phys. Rev. B **69**, 125324 (2004).
[40]Y. Ono, K. Nishiguchi, A. Fujiwara, H. Yamaguchi, H. Inokawa, and Y. Takahashi, Appl. Phys. Lett. **90**, 102106 (2007).
[41]M. A. H. Khalafalla, Y. Ono, K. Nishiguchi, and A. Fujiwara, Appl. Phys. Lett. **94**, 223501 (2009).
[42]M.A.H. Khalafalla, Y. Ono, K. Nishiguchi, and A. Fujiwara, Appl. Phys. Lett. **91**, 263513 (2008).
[43]M. Pierre, R. Wacquez, X. Jehl, M. Sanquer, M. Vinet, and O. Cueto, Nat. Nanotechnol. **5** 133 (2010).
[44]H. Sellier, G.P. Lansbergen, J. Caro, S. Rogge, N. Collaert, I. Ferain, M. Jurczak, and S. Biesemans, Phys. Rev. Lett. **97**, 206805 (2006).
[45]K. Y. Tan, K. W. Chan, M. Möttönen, A. Morello, C. Yang, J. van Donkelaar, A. Alves, J.-M. Pirkkalainen, D. N. Jamieson, R.G. Clark, and A. S. Dzurak, Nano Lett. **10**, 22 (2010).
[46]L. E. Calvet, W. Wernsdorfer, J. P. Snyder, and M. A. Reed, J. Phys. Condens. Matter **20**, 374125 (2008).
[47]C. Wang, Ph.D. thesis, University of Illinois at Urbana-Champaign, 1998.
[48]O. Makarovsky, O. Thomas, A. G. Balanov, L. Eaves, A. Patanè, R. P. Campion, C. T. Foxon, E. E. Vdovin, D. K. Maude, G. Kiesslich, and R. J. Airey, Phys. Rev. Lett. **101**, 226807 (2008).
[49]O. Makarovsky, A. G. Balanov, L. Eaves, A. Patanè, R. P. Campion, C. T. Foxon, and R. J. Airey, Phys. Rev. B **81**, 035323 (2010).
[50]R. M. Potok, J. A. Folk, C. M. Marcus, V. Umansky, M. Hanson, and A. C. Gossard, Phys. Rev. Lett. **91**, 16802 (2003).
[51]I. Kuljanishvili, C. Kayis, J. F. Harrison, C. Piermarocchi, T. A. Kaplan, S. H. Tessmer, L. N. Pfeiffer, and K. W. West, Nat. Phys. **4**, 227 (2008).
[52]A. K. Geim, T. J. Foster, A. Nogaret, N. Mori, P. J. McDonnell, N. La Scala Jr., P. C. Main, and L. Eaves, Phys. Rev. B **50**, 8074 (1994).
[53]A. K. Savchenko, V. V. Kuznetsov, A. Woolfe, D. R. Mace, M. Pepper, D. A. Ritchie, and G. A. C. Jones, Phys. Rev. B **52**, R17021 (1995).
[54]V. V. Kuznetsov, A. K. Savchenko, M. E. Raikh, L. I. Glazman, D. R. Mace, E. H. Linfield, and D. A. Ritchie, Phys. Rev. B **54**, 1502 (1996).
[55]V. V. Kuznetsov, A. K. Savchenko, D. R. Mace, E. H. Linfield, and D. A. Ritchie, Phys. Rev. B **56**, R15533 (1997).
[56]J. König and Y. Gefen, Phys. Rev. B **65**, 045316 (2002).
[57]F. Marquardt and C. Bruder, Phys. Rev. B **68**, 195305 (2003).
[58]S. Tanaka, M. Kobayashi, E. Hanamura, and K. Uchinokura, Phys. Rev. **134**, A256 (1964).
[59]A. Kormányos, I. Grace, and C. J. Lambert, Phys. Rev. B **79**, 075119 (2009).